Transient competitive complexation in biological kinetic isotope fractionation explains non-steady isotopic effects: Theory and application to denitrification in soils

Federico Maggi[a] and William J. Riley[b]

[a]Berkeley Water Center, Civil and Environmental Engineering, 413 O'Brien Hall, University of California, Berkeley, CA 94720-1710, USA.

[b]Earth Sciences Division, Lawrence Berkeley National Laboratory, Berkeley, CA 94720, USA.

Federico Maggi, fmaggi@berkeley.edu

Abstract.

The theoretical formulation of biological kinetic reactions in isotopic applications often assume first-order or Michaelis-Menten-Monod kinetics under the quasi-steady-state assumption to simplify the system kinetics. However, isotopic effects have the same order of magnitude as the potential error introduced by these simplifications. Both formulations lead to a constant fractionation factor which may yield incorrect estimations of the isotopic effect and a misleading interpretation of the isotopic signature of a reaction. We have analyzed the isotopic signature of denitrification in biogeochemical soil systems by Menyailo and Hungate [2006], where high $^{15}N_2O$ enrichment during N_2O production and inverse isotope fractionation during N_2O consumption could not be explained with first-order kinetics and the Rayleigh equation, or with the quasi-steady-state Michaelis-Menten-Monod kinetics. When the quasi-steady-state assumption was relaxed, transient Michaelis-Menten-Monod kinetics accurately reproduced the observations and aided in interpretation of experimental isotopic signatures. These results may imply a substantial revision in using the Rayleigh equation for interpretation of isotopic signatures and in modeling biological kinetic isotope fractionation with first-order kinetics or quasi-steady-state Michaelis-Menten-Monod kinetics.

1. Introduction

Isotope techniques have been used in a number of studies to characterize point- and ecosystem-scale sources and sinks of tracers such as gaseous NO, N_2O, and CO_2 and aqueous NH_4^+, NO_2^-, and NO_3^- [e.g., Mosier, 1998; Vitousek et al., 1997; Perez *et al.*, 2006]. Analysis of the isotopic signature of N compounds in ecological systems has traditionally been based on the Rayleigh (distillation) equation, which relates the transient isotope composition of substrate and product to a fractionation factor α under the assumption that the reactions are first order [Mariotti *et al.*, 1981]. This assumption is often not satisfied in soil systems as the largest part of soil nutrient cycling, driven by microorganisms via enzymatic reactions, has been more generally observed to follow Michaelis-Menten kinetics with the biomass following Monod kinetics. The magnitude of potential errors introduced by inappropriate application of first-order kinetics calls into question the assumptions invoked in point-scale modeling and interpretation of isotopic measurements that use the Rayleigh equation.

Recent experiments presented in Menyailo and Hungate [2006] and Toyoda *et al.* [2005] showed interesting results of the ^{15}N isotope composition of nitrous oxide, $\delta^{15}N_2O$, measured during denitrification in sampled soil systems. Focusing on Menyailo and Hungate results, $\delta^{15}N$ values derived with the Rayleigh equation underestimated the observed high isotope enrichment during N_2O production, while an inverse fractionation (preference for heavy isotopes) was observed during N_2O consumption and could not be predicted by the Rayleigh equation. To improve the understanding of these observations in terms of chemical kinetics the Michaelis-Menten-Monod kinetics can be invoked. However, it is not suf-

ficient to describe isotopic effects with the classic Michaelis-Menten-Monod kinetics. The approach to simplify the Michaelis-Menten-Monod kinetics employs the quasi-steady-state assumption during complexation of substrate and enzyme. By using this assumption in a competitive complexation system where the competing compounds are isotopologues, the fractionation factor becomes invariant [e.g., Hunkeler and Aravena, 2000] and, therefore, cannot explain the inverse fractionation observed during N_2O consumption.

We propose here the following hypothesis: biological kinetic isotope fractionation in competitive complexation reactions follows transient Michaelis-Menten-Monod kinetics and the resulting fractionation factor α is not invariant but depends on substrate and complex isotopic compositions. The transient assumption, which replaces the quasi-steady-state assumption, does not yield a simplified analytic form for substrates, complexes, products and microbial concentrations. However, it allows for a variable α and provides an explanation of the experimental observations of Menyailo and Hungate [2006].

The aim of this work is to develop the mathematics to describe microbially-mediated isotopic reactions and to test whether the hypothesis of transient Michaelis-Menten-Monod kinetics can aid in interpreting the isotopic signatures in biogeochemical systems. To this end, we compared modeling results using first-order kinetics and the corresponding Rayleigh approximation equation, and Michaelis-Menten-Monod kinetics under both quasi-steady-state and transient assumptions. The components' concentrations, isotopic compositions, and fractionation factors presented here were computed with each model and compared with the experimental observations of Menyailo and Hungate.

The approach presented here for the first time allows predictions of isotopic effects that would not otherwise be detectable using first-order kinetics and quasi-steady-state

Michaelis-Menten-Monod kinetics and has wider implications for the description of the kinetics of competitive isotopologues kinetics in enzymatic reactions in general. Furthermore, solving the transient Michaelis-Menten-Monod kinetics does not add complexity to the governing equations and has comparable costs to solving the quasi-steady-state kinetics.

2. Theory

In this section we review the fundamentals of first-order kinetics and quasi-steady-state Michaelis-Menten-Monod kinetics previously used to describe isotope fractionation. We then show how transient Michaelis-Menten-Monod kinetics overcome several limitations imposed to substrate, complex, and enzyme concentrations by first-order and quasi-steady-state kinetics.

2.1. First-order kinetic isotope fractionation and the Rayleigh equation

First-order (FO) kinetics have found a wide application, especially in the last two decades, in environmental disciplines related to nutrient biogeochemical cycling in soils. The principle of FO kinetics in isotope modeling is based on the uncoupled kinetic reactions

$$\mathrm{S} \xrightarrow{k} \mathrm{P}, \qquad \mathrm{S}' \xrightarrow{k'} \mathrm{P}' \tag{1}$$

which describe simultaneous transformation of the isotopologue substrates S and S' into the corresponding products P and P' at rates k and k'. Under the hypothesis that the system is closed, i.e., $S(t) + P(t) = S_0$ and $S'(t) + P'(t) = S'_0$, where S_0 and S'_0 are the initial substrate concentrations, the first-order kinetics describing the rates of change of

S, S', P and P' are

$$\frac{\mathrm{d}S}{\mathrm{d}t} = -\frac{\mathrm{d}P}{\mathrm{d}t} = -kS, \quad \frac{\mathrm{d}S'}{\mathrm{d}t} = -\frac{\mathrm{d}P'}{\mathrm{d}t} = -k'S' \tag{2}$$

with analytical solutions

$$S(t) = S_0 e^{-kt}, \quad S'(t) = S'_0 e^{-k't}, \tag{3}$$

$$P(t) = S_0(1 - e^{-kt}), \quad P'(t) = S'_0(1 - e^{-k't}). \tag{4}$$

Equations. (2) can be used to define the instantaneous isotope product composition R_{iP} =dP'/dP, and the accumulated isotope composition $R_P = P'/P$ and $R_S = S'/S$ for the product and substrate, respectively. The isotope compositions R_{iP} and R_S are used to define the isotope fractionation factor α [Mariotti *et al.*, 1981]

$$\alpha = \frac{R_{iP}}{R_S} = \frac{\mathrm{d}P'}{\mathrm{d}P} \Big/ \frac{S'}{S}, \tag{5}$$

which becomes

$$\alpha = \frac{\mathrm{d}P'}{\mathrm{d}P} \Big/ \frac{S'}{S} = k'/k = \text{const}, \tag{6}$$

upon substitution of Eqs. (2). Integration of Eq. (6) for dP' = −dS' and dP = −dS yields the Rayleigh equation describing $R_S(t)$ over time [Mariotti *et al.*, 1981]

$$R_S(t) \simeq R_{S,0} f(t)^{\alpha - 1}, \tag{7}$$

where $R_{S,0}$ is the initial substrate isotope composition, and $f(t) = S(t)/S_0$ is the fraction of remaining substrate. Because the system is closed (i.e., $S_0 = S(t) + P(t)$), the isotope composition of accumulated, R_P, and instantaneous, R_{iP}, products can be written as

$$R_P(t) \simeq R_{S,0} \frac{1 - f(t)^{\alpha}}{1 - f(t)}, \tag{8}$$

$$R_{iP}(t + dt) = \alpha R_S(t). \tag{9}$$

It is common to describe the isotope composition relative to a standard, R_{std}, as $\delta = (R/R_{std} - 1)1000$. Therefore, Eqs. (7), (8), and (9) become [Mariotti *et al.*, 1981]

$$\delta_S(t) \simeq \delta_{S,0} + \epsilon \ln[f(t)], \tag{10a}$$

$$\delta_P(t) \simeq \delta_{S,0} - \epsilon \frac{f(t) \ln[f]}{1 - f(t)}, \tag{10b}$$

$$\delta_{iP}(t + dt) \simeq \delta_S(t) + \epsilon, \tag{10c}$$

with $\epsilon = (\alpha - 1)1000$ the enrichment factor [Mariotti *et al.*, 1981]. Equations (2) and the Rayleigh approximations in Eqs. (10) have been used to interpret the isotopic signature in several biochemical reactions. The advantages in using FO kinetics lie in the model simplicity and the ability to derive exact solutions for $S(t)$, $S'(t)$, $P(t)$, $P'(t)$ and α, and approximate analytic solutions for the δ values as in Eqs. (10). However, FO kinetics and the Rayleigh equations are limited in isotope applications to biochemistry because substrate consumption is normally associated with microbial biomass dynamics and specific enzymes that compete for the substrates (i.e., the reactions are coupled) to form the products.

2.2. Quasi steady state Michaelis-Menten-Monod kinetic isotope fractionation

A richer description with respect to first-order kinetics was achieved by the 1913's Michaelis-Menten model [Laidler, 1955] where the substrate, S, was assumed to attach to an enzyme, E, to form a complex, C. In that work, the complex was assumed to be in fast equilibrium with S and E and to dissociate yielding the product, P, and releasing free, unchanged enzyme. Within our purpose of modeling isotopic effects, this approach leads to the two coupled reactions for S and S'

$$\mathrm{S{+}E} \underset{k_2}{\overset{k_1}{\rightleftarrows}} \mathrm{C} \xrightarrow{k_3} \mathrm{P} + \mathrm{E}, \qquad \mathrm{S'} + \mathrm{E} \underset{k_2'}{\overset{k_1'}{\rightleftarrows}} \mathrm{C'} \xrightarrow{k_3'} \mathrm{P'} + \mathrm{E}, \tag{11}$$

where k_i and k_i' are the rate constants corresponding to the isotopologue reactions.

In these reactions all stoichiometric coefficients have been taken equal to 1 while the concentrations of S, S', C, C', P, and P' have units of mass per gram of soil. For example, using the N nitrogen atom as the tracer of the denitrification reaction that produces N_2O from NO_3^-, S, C, and P are expressed in [mg N kg_{soil}^{-1}]. Identically, for the isotopologue reaction that produces $^{15}N^{14}NO$ from $^{15}NO_3^-$ and $^{14}NO_3^-$, S', C', and P' are also expressed in [mg N kg_{soil}^{-1}]. The isotopologue reaction that consumes $^{15}NO_3^-$ and $^{15}NO_3^-$ and produces $^{15}N^{15}NO$ is not included in reactions of Eq. (11) due to its scarsity. The same approach is used for the reaction that produces N_2 from N_2O.

The two reactions can be conveniently described by choosing the concentrations S, S', C, C' as independent variables. Assuming that the system is closed to mass transfer, the following mass conservation laws can be written

$$S_0 = S(t) + C(t) + P(t), \tag{12a}$$

$$S_0' = S'(t) + C'(t) + P'(t), \tag{12b}$$

$$E_0 = E(t) + C(t) + C'(t). \tag{12c}$$

where S_0, S_0', and E_0 are the initial substrate and enzyme concentrations. The mass balance for the substrate S has been simplified under the assumption that the transfer of light isotopes from the substrate S towards the heavy product P' does not appreciably affect the concentration of S. For example, the rate of consumption of $^{14}NO_3^-$ substrate is 1/2 the rate of production of $^{15}N^{14}NO$; because the isotopic ratio $^{15}N^{14}NO/^{14}N_2O$ is in the order of magnitude of 10^{-2}, the consumption of ^{14}N from $^{14}NO_3^-$ to form $^{15}N^{14}NO$ is

in the order of $5 \cdot 10^{-3}$ of the concentration of $^{14}NO_3^-$. Equation (12c) establishes that the two substrates S and S' compete to bound to the enzyme to form the complexes C and C', and is responsible for the coupling of the two reactions in Eq. (11).

In the approach presented here the enzyme concentration is assumed to be linearly proportional by a factor z to the biomass concentration B as

$$E(t) = zB(t). \tag{13}$$

Because B is assumed to increase in response to the release of P and P' over time according to the Monod model [Monod, 1949], Eq. (13) implies that the enzyme is synthesized at the same rate as biomass growth and deteriorates at the same rate as microbial cells die. This approach, though simplifying the enzyme dynamics, improves the original Michelis-Menten formulation by which E was considered constant and not linked to any microbial biomass dynamics.

Using the mass conservation laws in Eqs. (12), the kinetic equations for each component in the system of Eq. (11), including the biomass, can be written as follows

$$\frac{\mathrm{d}S}{\mathrm{d}t} = -k_1 SE + k_2 C, \tag{14a}$$

$$\frac{\mathrm{d}S'}{\mathrm{d}t} = -k_1' S'E + k_2' C', \tag{14b}$$

$$\frac{\mathrm{d}C}{\mathrm{d}t} = k_1 SE - (k_2 + k_3)C, \tag{14c}$$

$$\frac{\mathrm{d}C'}{\mathrm{d}t} = k_1' S'E - (k_2' + k_3')C', \tag{14d}$$

$$\frac{\mathrm{d}P}{\mathrm{d}t} = -\frac{\mathrm{d}S}{\mathrm{d}t} - \frac{\mathrm{d}C}{\mathrm{d}t} = k_3 C, \tag{14e}$$

$$\frac{\mathrm{d}P'}{\mathrm{d}t} = -\frac{\mathrm{d}S'}{\mathrm{d}t} - \frac{\mathrm{d}C'}{\mathrm{d}t} = k_3' C', \tag{14f}$$

$$\frac{\mathrm{d}E}{\mathrm{d}t} = z\frac{\mathrm{d}B}{\mathrm{d}t} - \frac{\mathrm{d}C}{\mathrm{d}t} - \frac{\mathrm{d}C'}{\mathrm{d}t}, \tag{14g}$$

$$\frac{\mathrm{d}B}{\mathrm{d}t} = Y\left(\frac{\mathrm{d}P}{\mathrm{d}t} + \frac{\mathrm{d}P'}{\mathrm{d}t}\right) - \beta B \tag{14h}$$

where Eq. (14h) is the Monod equation describing microbial biomass dynamics with Y the yield coefficient expressing the biomass gain per unit of released product and β expressing the biomass death rate [Monod, 1949].

A simplified expression for this system of eight ordinary differential equations in eight unknowns can be obtained assuming that complexation of C and C' is very fast at the early stage of the reactions, and that, afterwards, their concentrations do not change appreciably in time. This assumption, known as Haldane-Briggs, is commonly referred to as quasi steady state [Haldane, 1930; Laidler, 1955], and implies that C and C' are small and that

$$\frac{\mathrm{d}C}{\mathrm{d}t} \simeq 0, \qquad \frac{\mathrm{d}C'}{\mathrm{d}t} \simeq 0. \tag{15}$$

Substituting Eqs. (15) into Eqs. (14e), (14f), and (14g), the quasi-steady-state assumption also implies

$$\frac{\mathrm{d}S}{\mathrm{d}t} \simeq -\frac{\mathrm{d}P}{\mathrm{d}t}, \quad \frac{\mathrm{d}S'}{\mathrm{d}t} \simeq -\frac{\mathrm{d}P'}{\mathrm{d}t}, \quad \frac{\mathrm{d}E}{\mathrm{d}t} \simeq z\frac{\mathrm{d}B}{\mathrm{d}t}. \tag{16}$$

Introducing Eqs. (12) into Eqs. (14c) and (14d) under the quasi-steady-state assumption, the kinetic equations for C and C' become

$$\frac{\mathrm{d}C}{\mathrm{d}t} = k_1 S(zB - C - C') - (k_2 + k_3)C \simeq 0, \tag{17a}$$

$$\frac{\mathrm{d}C'}{\mathrm{d}t} = k_1' S'(zB - C - C'), -(k_2' + k_3')C' \simeq 0, \tag{17b}$$

and can be solved for C and C' to yield

$$C \simeq \frac{zBS}{S + K(1 + S'/K')}, \quad C' \simeq \frac{zBS'}{S' + K'(1 + S/K)}, \tag{18}$$

with $K = (k_2 + k_3)/k_1$ and $K' = (k_2' + k_3')/k_1'$ the Michaelis-Menten parameters (or half-saturation concentrations) [Haldane, 1930]. In the classic approach to solve the Michaelis-Menten kinetics with the Haldane-Briggs' quasi-steady-state assumption, the total enzyme concentration (free plus bound in the complexes) E_t = constant appears in place of the transient product zB in the numerators of Eq. (18) of our approach. Introducing the approximate solutions for C and C' of Eq. (18) into Eqs. (14e), (14f), and (14h), and using Eqs. (16), we obtain

$$\frac{\mathrm{d}P}{\mathrm{d}t} \simeq k_3 \frac{zBS}{S + K(1 + S'/K')}, \tag{19a}$$

$$\frac{\mathrm{d}P'}{\mathrm{d}t} \simeq k_3' \frac{zBS'}{S' + K'(1 + S/K)}, \tag{19b}$$

$$\frac{\mathrm{d}S}{\mathrm{d}t} \simeq -\frac{\mathrm{d}P}{\mathrm{d}t}, \tag{19c}$$

$$\frac{\mathrm{d}S'}{\mathrm{d}t} \simeq -\frac{\mathrm{d}P'}{\mathrm{d}t}, \tag{19d}$$

$$\frac{\mathrm{d}B}{\mathrm{d}t} \simeq \frac{k_3 Y zBS}{S + K(1 + S'/K')} + \frac{k_3' S' Y zB}{S' + K'(1 + S/K)} - \beta B, \tag{19e}$$

which are normally known as the Michaelis-Menten kinetics with biomass dynamics following Monod kinetics. From here on we will call this approach with the acronym QSS-MMM kinetics to highlight that the Michaelis-Menten-Monod kinetics are solved under the assumption of quasi steady state.

Introducing $\mathrm{d}P$ and $\mathrm{d}P'$ of Eqs. (19a) and (19b) into Eq. (5) for the fractionation factor α we obtain

$$\alpha = \frac{\mathrm{d}P'}{\mathrm{d}P} \Big/ \frac{S'}{S} \simeq \frac{k_3'}{k_3} \frac{S + K(1 + S'/K')}{S' + K'(1 + S/K)} = \frac{k_3' K}{k_3 K'} = \text{constant} \tag{20}$$

In this case, however, Eqs. (19a) and (19b) cannot be integrated analytically so no approximation for the δ^{15}N can be derived as was done for the Rayleigh approximation equations.

The approximate solutions of Eqs. (19) to the system of differential equations in Eqs. (14), achieved using the Haldane-Briggs' quasi-steady-state assumption, imply that $CK \simeq SE$ and $C'K' \simeq S'E$ over the entire reaction course. The circumstances under which these conditions are valid are that C and C' have to be small and time invariant (Eqs. (15)). For C and C' to be small the conditions $C \ll S$ and $C' \ll S'$ have to be satisfied. Consequently, the K and K' values have to be large numbers on the same order of magnitude as S and S' (i.e., $S \sim K$ and $S' \sim K'$), while the free enzyme concentration E has to be a small number on the same order of magnitude as C and C' (i.e., $E \sim C \sim C'$). While these conditions may be encountered in common enzymatic reactions, the boundaries of validity in isotopic applications become more restrictive. If the $'$ refers to rare isotopologues with natural abundance (i.e., $S \gg S'$, $C \gg C'$, and $K \simeq K'$) and if $S \sim K \simeq K'$, then it must be $S' \ll K'$. This relation poses a first limitation to

the quasi-steady-state assumption which requires $S' \sim K'$. In addition, if $E \sim C$, then it must be $E \gg C'$ whereas $E \sim C'$ is expected for assuming quasi steady state. This second condition that applies to E, C, and C' strongly limits the quasi-steady-state assumption because in our modeling development we have assumed that the enzyme concentration is not constant but varies with biomass concentration. In instances where the biomass concentration increases, and in so doing the free enzyme concentration increases too, the system may depart from the condition $E \sim C \sim C'$ (i.e., $E > C \gg C'$), worsening the degree of applicability of quasi steady state. Conversely, in instances where the free enzyme concentration decreases, the system may meet only one of the conditions $E \sim C$ or $E \sim C'$.

2.3. Transient kinetic isotope fractionation

Regardless of the fact that isotopic effects measured in natural-abundance biochemical reactions are normally very small (i.e., $\alpha \approx 1$), the isotopic effects modeled with either first-order kinetics or quasi-steady-state Michaelis-Menten-Monod kinetics have as outcome a constant isotopic effect. This constancy implies that, for stable isotopologues, biochemical reactions always produce depleted products while enriching the remaining substrates owing to the preference of enzyme systems to use lighter isotopologue substrates. In the case of first-order kinetics and quasi-steady-state Michaelis-Menten-Monod kinetics this is a straightforward conclusion from Eqs. (6) and (20), as the substrate is directly transformed into a product (i.e., $\mathrm{d}P = -\mathrm{d}S$ and $\mathrm{d}P' = -\mathrm{d}S'$) or, equivalently, the complexation rate is null (i.e., $\mathrm{d}C = \mathrm{d}C' = 0$). If, however, the quasi-steady-state Haldane-Briggs hypothesis is not used to solve the Michaelis-Menten-Monod kinetics (i.e., $\mathrm{d}C \neq 0$ and $\mathrm{d}C' \neq 0$), a different conclusion is reached. The isotoplogue substrates S

and S', while competing to bond to the enzyme without conditions imposed on the concentrations discussed above, will form reversible complexes that will either accumulate, decompose back to substrates, or release products. Along each of these pathways, the isotopic fractionation changes the isotope composition of the total substrate $S(t) + S'(t)$, complex $C(t) + C'(t)$, and product $P(t) + P'(t)$ over time. This fractionation sequence is further fed by the feedback introduced by the concentration of free enzyme, which is synthesized by microbes that grow at the rate at which the products are released (i.e., proportional to k_3 and k_3') and affects the rate at which the substrates bind in the complexes (i.e., proportional to k_1 and k_1'). The quasi-steady-state assumption applied to C and C' is invoked to achieve a simplified expression of these kinetics but does not allow quantitative treatment of these effects, which, although small in absolute terms, have the same order of magnitude (one part per thousand) as the fractionation factor. It is therefore meaningful to challenge the quasi-steady-state assumption and question whether doing so could bring to light nonlinear effects during transient complexation in microbially-induced isotope fractionation modelled with Michaelis-Menten-Monod kinetics.

By relaxing the quasi-steady-state assumption in Eq. (15), the system kinetics in Eqs. (14) cannot be re-written in a simplified form as Eqs. (19). We name the full set of differential equations in Eqs. (14) with the acronym TR-MMM to underline that it is solved for the transient kinetics.

An expression for α can be derived by combining Eqs. (14e) and (14f) as follows

$$\alpha(t) = \frac{\mathrm{d}P'}{\mathrm{d}P} \Big/ \frac{S'}{S} = \frac{\mathrm{d}S' + \mathrm{d}C'}{\mathrm{d}S + \mathrm{d}C} \Big/ \frac{S'}{S} = \frac{k_3' C'}{k_3 C} \frac{S}{S'} = \frac{k_3'}{k_3} \frac{R_C(t)}{R_S(t)}. \tag{21}$$

This expression for α shows that in the most general case of biological kinetic isotope fractionation, the isotopic effect may change with the substrate concentrations S and S' and complex concentrations C and C', and can be re-written in terms of isotope compositions R_C and R_S. Equation (21), derived without imposing conditions on complex dynamics, generalizes the fractionation factor derived for quasi-steady-state Michaelis-Menten-Monod kinetics in Eq. (19). Because Eqs. (14e) and (14f) do not have an analytic solution, the Rayleigh approximation equations cannot be derived as for the case of quasi-steady-state Michaelis-Menten-Monod kinetics (Section 2.2).

3. Results

3.1. Experimental data

The experimental data used in this work were collected in incubated soils taken from under larch trees during denitrification, i.e., along the reaction $NO_3^- \rightarrow N_2O \rightarrow N_2$, and previously published in Menyailo and Hungate [2006]. The values of $\delta^{15}N_2O$ were measured during N_2O production from NO_3^- using N_2O-reductase acetylene inhibition [e.g., Groffman *et al.*, 2006] and, separately, during N_2O consumption into N_2. The available data from Menyailo and Hungate [2006] are the N_2O concentrations over time during both N_2O production and consumption, and the $\delta^{15}N_2O$ values over time and as a function of the substrate concentration, the latter being estimated from the product concentration in the test of N_2O production. The data sets of N_2O and $\delta^{15}N_2O$ over time (see Figures 1 and 3) were used to test our hypothesis by using the three models described in Section 2: (*i*) first-order (FO) kinetics and the corresponding Rayleigh approximation equations; (*ii*) the quasi-steady-state Michaelis-Menten-Monod kinetics (QSS-MMM), and (*iii*) transient Michaelis-Menten-Monod kinetics (TR-MMM).

3.2. Model calibration

Calibration of the three models was carried out with measured N_2O concentration and with the $\delta^{15}N_2O$ as a function of time in both production and consumption tests. All modeling predictions presented here were computed by numerically solving the kinetics of each system component with an explicit finite difference technique. The optimal parameter values were calculated using the software package PEST (Parameter ESTimation, Papadopulos & Associates Inc., www.sspa.com/pest) by minimization of the difference between experimental and simulated values. For each model, several calibrations were run starting from different initial values of the parameters to assure that the optimal sets were unique. The enzyme yield coefficient, $z = 0.01$, was arbitrary chosen knowing that the ratio E/B is small, while the microbial death rate, β, and the yield coefficient, Y, were iteratively computed in this multiple calibration process and were held identical in the QSS-MMM and TR-MMM kinetics assuming that the denitrifier bacteria were the same in both N_2O production and consumption tests. Similarly, all initial conditions were kept identical in the three models (Table 1). Calibration of the rate constants k_i and k'_i of the QSS-MMM and TR-MMM models was carried out under the constraints $k'_i < k_i$. These constraints were taken under the hypothesis that all reactions pathways involving the rare (heavier) isotopologues (S', C', and P') required a slightly higher amount of energy with respect to the reactions involving the abundant (lighter) isotopologues, as discussed in Section 4.

3.3. Parameters analysis

It is interesting to note from Table 1 that k and k' values for FO kinetics have the same order of magnitude in the two tests of N_2O production and consumption (10^{-6} s^{-1}). This

pattern also occurs for k_3 and k_3' in the QSS-MMM and TR-MMM kinetics, which had the same order of magnitude during N_2O production and consumption (10^{-4} s^{-1}). The most important feature was the persistent pattern found for the Michaelis-Menten parameters K and K' in the QSS-MMM kinetics, whose values were approximately 70 and 150 mg kg_{soil}^{-1} for N_2O production and consumption, respectively, and in the TR-MMM kinetics (i.e., K and K' markeed with star in Table 1), whose values were about 100 mg kg_{soil}^{-1} for both N_2O production and consumption tests. These values were also close to values of ≈ 100 mg kg_{soil}^{-1} reported in Li *et al.* [1992]. This feature anticipates that the QSS-MMM and TR-MMM kinetics were coherent with each other, and were nearly equivalent in terms of reaction rates and enzyme-substrate affinity.

3.4. N_2O production

During N_2O production, predictions of N_2O concentration using FO kinetics, Eqs. (2), deviated from the measurements and underestimated $\delta^{15}N_2O$ from time $t > 20$ h and as a function of consumed substrate $(1 - f)$ (solid gray line in Figure 1). Use of the Rayleigh approximation in Eq. (10b) to predict $\delta^{15}N_2O$ as a function of $(1 - f)$ with the parameters reported in Table 1 resulted in a better fit as compared to the results shown in Menyailo and Hungate [2006] (dot-dashed gray line and dot-dashed black line, respectively, in Figure 1*c*).

Predictions using the Micaelis-Menten-Monod kinetics, Eqs. (19) and Eqs. (14), matched the N_2O concentration and the $\delta^{15}N_2O$ values over time with higher accuracy than FO kinetics. QSS-MMM and TR-MMM kinetics were also nearly equivalent in that the modeled curves were almost overlapping in all panels of Figure 1. The rates of change dC and dC' suggest that complexation played a role in this reaction (Figure 1*a*). However,

the complex concentrations were smaller than those of the substrates for the largest part of the measurement (i.e., $C \ll S$ and $C' \ll S'$); this explained why the approximation introduced by the quasi-steady-state assumption did not substantially affect the capability of QSS-MMM kinetics to replicate the N_2O production observations.

An inspection of the fractionation factor α shows that FO and QSS-MMM kinetics yielded steady isotopic effects (i.e., $\alpha \approx 0.983$ and $\alpha \approx 0.979$, respectively), while TR-MMM kinetics led to a slightly non-steady isotopic effect with α increasing and decreasing just below $\alpha \approx 0.981$ (Figure 2).

Though underestimating the measured data points in Figure 1*c*, the three models tested here gave better predictions of $\delta^{15}N_2O$ as a function of the fraction of consumed substrate than the Rayleigh approximation proposed in Menyailo and Hungate [2006]. To explain this mismatch, Menyailo and Hungate invoked (*i*) an incorrect estimation of the remaining substrate concentration f (because of immobilization or, for any reason, substrate not fully available to denitrifiers) or (*ii*) a decline in isotopic enrichment as the substrate became limiting. The fact that Michaelis-Menten-Monod kinetics accurately predicted N_2O concentration and $\delta^{15}N_2O$ over time (Figure 1*a* and *b*) shows that hypothesis (*i*) was true to the extent to which the measured $\delta^{15}N_2O$ values departed from the curves obtained with our models in Figure 1*c*. This distance, measured along the x-coordinate, is an estimate of the error in the measurement of the fraction of consumed substrate $(1 - f)$ as hypothesized in (*i*) by Menyailo and Hungate [2006]. Furthermore, hypothesis (*ii*) was also relatively correct in that a decline in isotopic enrichment corresponded to an increased fractionation factor, the behavior that was reproduced by TR-MMM kinetics in the first 40 h of the simulation (Figure 2).

3.5. N_2O consumption

We repeated analogous simulations for the experiment of N_2O consumption. Also in this case, Michaelis-Menten-Monod kinetics reproduced the substrate N_2O concentration and $\delta^{15}N_2O$ over time and as a function of f more accurately than FO kinetics and the Rayleigh approximation equations (Figure 3a, b and c). However, differently from FO and QSS-MMM kinetics, TR-MMM kinetics could replicate the initially high N_2O enrichment in ^{15}N in the first 80 hours of observations, and the later inverse isotopic effect that depleted the N_2O substrate (Figures 3b and c).

To explain the inverse isotopic effect (i.e., preference for the heavier isotopologue), Menyailo and Hungate invoked the presence of another enzyme system that became active late in the incubation. If this hypothesis is taken as true along with the first-order kinetics assumption which assumes that $\alpha < 1$, then one mechanism possibly contributing to inverse fractionation would have implied production of depleted N_2O (no $^{15}N_2O$) from some substrate. Because the decrease is $\Delta\delta^{15}N_2O \approx 10‰$, the decrease in substrate isotopic composition is $\Delta R_S = {}^{15}N_2O/\Delta^{14}N_2O \approx 0.0233$, with $R_{std} = 2.305 \cdot 10^{-2}$. This implies a $\Delta^{14}N_2O \approx 40\,{}^{15}N_2O$. Because the $^{15}N_2O$ concentration from time $t = 80$ h was always smaller than 15 mg N-N_2O kg_{soil}^{-1} and never lower than 3 mg N-N_2O kg_{soil}^{-1} (not shown), we infer that the increase in bulk N_2O concentration associated with this proposed additional enzyme system should have been in the range 100-600 mg N-N_2O kg_{soil}^{-1} higher than the one observed in Figure 3a, while the experiments did not show such an increase. Excluding therefore any concurrent mechanism of N_2O production, the analysis of the fractionation factor (Figure 4) showed more clearly that TR-MMM kinetics could replicate inverse isotopic effects owing to α increasing from less than 0.99 to more

than 1.01, with a crossover to values larger than 1 occurring at time $t \simeq 80$ h (Figure 4). Conversely, FO and QSS-MMM kinetics always yielded constant α, with values $\alpha \simeq 0.998$. Because the fractionation factor in transient kinetics is $\alpha = (k'_3/k_3)(R_C/R_S)$, with $k'_3 < k_3$ from our calibration (see Table 1), inverse fractionation occurred when $R_S/R_C \leq k'_3/k_3 < 1$. These conditions occurred because of how the heavy isotopologue kinetics governed the rates of change of R_S and R_C ratios over time. These dynamics are as important for determining α as the fact that the complex concentrations C and C', though small compared to S and S', changed over time with a rate that could not be neglected, as discussed in Section 3.7.

3.6. Monte Carlo sensitivity analysis of TR-MMM kinetics

To characterize the sensitivity of the TR-MMM kinetics to its parameters, we performed a Monte Carlo analysis for N_2O production and consumption. We applied three independent normally-distributed probability density functions to the rate constant k'_i with averages obtained from calibration (Table 1) and standard deviation equal to 5‰ of each k'_i parameter, and limited to ± 3 times the standard deviation (600 replicates were sufficient to achieve steady distributions).

N_2O concentrations did not show appreciable impact from these distributions (data not shown). Conversely, $\delta^{15}N$ values were more sensitive, with a maximum standard deviation of approximately ± 5‰ and ± 18‰ during N_2O production and consumption, respectively (thin lines in Figure 5*a*). The standard deviation of the modeled $\delta^{15}N_2O$ values varied in time. Yet, while it was nearly constant at $\approx \pm 2$‰ around the average $\delta^{15}N_2O$ during N_2O production, it increased monotonically over time during N_2O consumption. This behavior was not observed in the standard deviation of the α values (Figure 5*b*), which was nearly

steady at approximately ±5‰ around the average α values in both N_2O production and consumption tests (Figure 5*b*). An analogous Monte Carlo analysis performed on the FO kinetics resulted in approximately ±4‰ maximum standard deviation in the $\delta^{15}N_2O$ values during N_2O production and consumption, and less than ±2‰ in the α values (data not shown).

A similar Monte Carlo sensitivity analysis was performed for the two microbial biomass parameters z, β, and Y which were described by three independent normally-distributed probability density functions with averages obtained from calibration (Table 1) and standard deviation equal to ±1% of each parameter. The standard deviation of the modeled $\delta^{15}N_2O$ values computed with the TR-MMM kinetics was less than 1‰ during N_2O production and reached a maximum of approximately ±4‰ during N_2O consumption (Figure 5*c*). Also in this case, the standard deviation in the $\delta^{15}N$ values was progressively amplified over time during N_2O consumption. The standard deviation in the modeled fractionation factor was negligible during N_2O production and reached a maximum of approximately ±10‰ during N_2O consumption (Figure 5*d*).

In this analysis we tested also the sensitivity to the initial isotopic compositions. In both experiments of N_2O production and consumption we noted that any increase or decrease in initial substrate isotopic composition was conservatively transferred to the product (data not shown).

3.7. Relative isotopic composition of complex and products in TR-MMM kinetics

An analysis of the time evolution of the complex and product isotopic composition was carried out by computing the ratios $R_C = C'/C$ and $R_P = P'/P$ relative to the substrate,

$R_S = S'/S$. During N_2O production, the product relative isotopic composition, R_P/R_S, experienced an initial enrichment, and a more important depletion afterwards (Figure 6*a*). These dynamics were accompanied by an enrichment of the complex relative isotopic composition, R_C/R_S, between 30 and 40 hours. Over all, the isotopic composition of complex and product N_2O remained smaller than 1, that is, depleted with respect to the substrate isotopic composition. Further, the complex relative composition, R_C/R_S, in the fractionation factor α of Eq. (21) never became larger than k_3/k'_3, meaning that α was always smaller than 1.

During N_2O consumption (Figure 6*b*), the complex relative isotopic composition R_C/R_S increased to values larger than 1 almost immediately after the reaction started, and remained larger than 1 during the entire reaction course. The product relative isotopic composition, R_P/R_S, remained smaller than one for the entire experiment (Figure 6*b*). Inverse fractionation observed in Figure 3*b* is mainly characterized by a depletion in N_2O substrate and N_2 product isotopic composition, and by an overall enrichment of the complex isotopic composition. Inverse fractionation occurred when the complex relative isotopic composition passed above the solid line that represents the ratio k_3/k'_3 and sets the threshold above which α becomes larger that 1 (Figure 6*b*).

3.8. Net and relative rates of change of substrate, complex, and products in TR-MMM kinetics

The net rates of change of substrate, complex, and product concentrations in the N_2O production and consumption experiments showed common features, with S and P characterized by an initial increase and a subsequent decrease (in absolute terms), while C was initially accumulated in the system, and then consumed to extinction (data not shown).

Similar trends were found for the heavy isotopologues S', C', and P' in both N_2O production and consumption experiments (data not shown). The rates of changes of the light isotopologues (dS, dS, and dP) were approximately 40 to 50 times higher relative to those of the heavy isotopologues (dS', dS', and dP') during N_2O production and consumption (Figure 7*a* and *b*). Regardless of the specific test, the relative rates of change of the substrates (dS/dS') and products (dP/dP') were always very similar. The relative rates of change of the complexes (dC/dC') underwent a singularity when C and C' started being consumed, i.e., dC/dC' jumped from $-\infty$ to $+\infty$ when dC'/dt crossed zero.

3.9. Phase space analysis

The microbial biomass dynamics drives the kinetic reactions and isotope fractionation, and is subject to a feedback linking the rate of change of S and S' to the rate of production of P and P' through the production of the enzyme E that forms the complexes C and C'. In the tests of N_2O production and consumption, the correlation between the microbial biomass and complex concentrations B and C normalized to their maxima were nearly always positive, with C increasing and decreasing with B, and a phase lag in the N_2O production experiment slightly larger than in the N_2O consumption (i.e., the solid ring is wider than the dash-dotted one, Figure 8*a*).

Conversely, the correlation between the normalized biomass concentration and the $\delta^{15}N_2O$ values showed very different patterns in the two tests (Figure 8*b*). These differences were due to the fact that $\delta^{15}N_2O$ always increased during N_2O production, while during N_2O consumption it increased first, and decreased next. It is interesting to note that during N_2O consumption (dashed-dot line), the maximum $\delta^{15}N$ value occurred nearly in concomitance with the maximum complex and biomass concentrations (Figure 8*b*). Af-

ter this point, $\delta^{15}N_2O$ decreased due to an inversion of isotopic effect ($\alpha > 1$) (Figure 8*c*).

4. Discussion

The results presented here highlighted three important aspects.

First, as compared to first-order reactions, improved predictions of substrate and product concentrations during N_2O production and consumption were achieved using Michaelis-Menten reactions coupled with Monod kinetics for the microbial biomass dynamics and the enzyme concentration. More importantly, this modeling framework was, in general, highly accurate in describing high enrichment in δ values during N_2O production and inverse fractionation during N_2O consumption without invoking additional processes that were not monitored in the experiments, and without introducing the constraints associated with the quasi-steady-state assumption. We do not exclude that other processes may partly have contributed to the observed isotopic effects. Among them, as suggested also in Menyailo and Hungate [2006], high enrichment during N_2O production and inverse fractionation during N_2O consumption could be ascribed to reactions occurring along the chain $NO_3^- \rightarrow NO_2^- \rightarrow NO \rightarrow N_2O$ [Knowles, 1982], nitrifier denitrification which may not be inhibited by C_2H_2 application [Menyailo and Hungate, 2006], and N-site isotopomer-specific fractionation, [Toyoda *et al.*, 2005]. However, we do not have measurements of these processes to assess their possible contributions; further experimental investigation would benefit our, and other, mathematical models.

Second, in contrast to the quasi-steady-state assumption, the transient assumption in Michaelis-Menten-Monod kinetics improved our ability to predict non-steady isotopic effects. With this assumption the fractionation factor α varied over the reaction, and was

not limited to values smaller than 1. This variability was linked to a changing isotopic composition of the complex and substrate over time, with the former playing a fundamental role in how rare isotopologues moved along the reaction pathway. It is important to note that inverse fractionation in biochemical reactions does not necessarily imply preference for (i.e., higher consumption rate of) lighter, abundant isotopologues over heavier, rare isotopologues. The relative rates of changes of the system components (Figure 7), and the reaction rate constants k_i and k_i' (Table 1), show that lighter isotopologues are always consumed more rapidly than heavier isotopologues. The reason why inverse fractionation may occur is related to the possibility for the heavy isotopologues to accumulate in the complex because its kinetics are not strictly described by equilibrium or steady-state kinetics. This added degree of freedom in biochemical reactions is possible only under the assumption of transient kinetics, by means of which the rate of complexation becomes non negligible. The transient hypothesis in solving the Michaelis-Menten-Monod kinetics has the advantage of generalizing the quasi-steady-state assumption without introducing approximations and constraints to the concentrations of the system components. We note that numerically solving the transient Michaelis-Menten-Monod kinetics for all components (i.e., heavy and light isotopologues, enzyme, and biomass) has comparable costs to solving the quasi-steady-state kinetics.

Third, a particular attention has to be payed to the thermodynamic description of the reaction rate constants k_i and k_i'. The rate constants obtained in our calibration were constrained to satisfy the conditions $k_i > k_i'$. Satisfaction of these conditions was taken on the basis of the hypothesis that the rate of a reaction, k, is exponentially dependent on

the energy barrier, E_a, that the reactants have to surpass to release the product according to the Arrhenius's law [Atkins, 1998]

$$k = Ae^{-E_a/RT}, \tag{22}$$

where A is a frequency factor with the unit that depends on the order of the reaction, T is the absolute temperature, and $R = 8.31$ J K^{-1} mol^{-1} is the constant for ideal gases. To follow the Arrhenius' law, the energy barrier E'_a linked to isotopically heavy reactants would be higher than the energy barrier E_a of isotopically light reactants owing to stronger atomic bonds in S' as compared to S. The constraint $k > k'$ implied therefore $E_a < E'_a$. Using the Arrhenius description of first-order reaction rates with the parameters of Table 1 for FO kinetics, and assuming that isotopic effects only relate to the energy barrier (i.e., the frequency factors are $A' = A$), the ratio $k'/k = e^{(E'_a - E_a)/RT}$ showed that the amount of surplus energy that heavy isotopologues substrates require to react in the FO kinetics approach, $(E'_a - E_a)$, was 42.05 and 6.86 J mol^{-1} for N_2O production and consumption, respectively. Because in the FO kinetics the ratio k'/k also equals the fractionation factor α of Eq. (6), we obtain that the isotopic effect is constant and equal to the exponent of the difference in energy barrier between heavy and light isotopologues as

$$\alpha = \frac{k'}{k} = \frac{A'}{A} e^{-(E'_a - E_a)/RT} = e^{-(E'_a - E_a)/RT},$$

under the assumption that $A' = A$. When the same approach was applied to the ratio of first-order rate constants k'_3/k_3 of the QSS-MMM kinetics, with $A' = A$, we obtained that $(E'_a - E_a)$ was 211.9 and 37.5 J mol^{-1} for N_2O production and consumption, respectively. In this instance the fractionation factor of Eq. (20),

$$\alpha = \frac{K}{K'}\frac{k_3'}{k_3} = \frac{KA'}{K'A}e^{-(E_a'-E_a)/RT} = \frac{K}{K'}e^{-(E_a'-E_a)/RT},$$

is proportional to the ratio K/K' and to the exponent of the difference in energy barrier between heavy and light isotopologues. For the TR-MMM kinetics, the ratio k_3'/k_3 implied that $(E_a' - E_a)$ was 40.68 and 268.61 J mol^{-1} for N_2O production and consumption, respectively. The fractionation factor of Eq. (21)

$$\alpha = \frac{R_C(t)}{R_S(t)}\frac{k_3'}{k_3} = \frac{R_C(t)}{R_S(t)}\frac{A'}{A}e^{-(E_a'-E_a)/RT} = \\ = \frac{R_C(t)}{R_S(t)}e^{-(E_a'-E_a)/RT},$$

showed that, for $A' = A$, the isotopic effect is proportional to an energy component that is constant in time (i.e., the exponential term) and to a time-changing ratio $R_C(t)/R_S(t)$.

Regardless of the accuracy in predicting the concentrations and isotopic compositions of all system components, the energy term $(E_a' - E_a)$ computed for N_2O production was variable between approximately 50 and 210 J mol^{-1}. In the test of N_2O consumption, instead, $(E_a' - E_a)$ ranged between approximately 7 and 270 J mol^{-1}. Although the variability found for $(E_a' - E_a)$ appears large, the activation energy (here coinciding with the Gibbs free energy) is about three orders of magnitude larger for N_2O production from NO_3^- (-390 kJ mol^{-1}) and for N_2O consumption into N_2 (-170 kJ mol^{-1}) [Sprent, 1987; Wrage et al., 2001]. It is interesting to note that the high difference in energy barrier found for N_2O consumption with the TR-MMM kinetics ($\approx$ 268 J mol^{-1}), which implies that the N_2 product is depleted in ^{15}N at a higher rate, does not necessarily imply that the N_2O substrate composition is enriched in ^{15}N. Because the quasi-steady state assumption is not used in the solution of the TR-MMM kinetics, both substrate and product can become

depleted at the expenses of the complex, which would be enriched. This nonlinear effect, expressed by the ratio $R_C(t)/R_S(t)$, depends on how the kinetics of each pathway in a competitive complexation reaction like those of Eq. (11) interact with each other.

If the isotopic effect in the above analysis is assumed to exclusively depend on the difference in activation energy $(E'_a - E_a)$ (i.e., the frequency factors $A' = A$), the transition state theory developed by Eyring allows us to take into account the isotopic effects related to A and A' [Eyring, 1935a, b]. The frequency factors for reactions in solution as in Eq. (11) can be written as [Connors, 1990]

$$A = \frac{K_B T}{h} \frac{F_C}{F_S F_E}, \qquad A' = \frac{K_B T}{h} \frac{F_{C'}}{F_{S'} F_E} \tag{24}$$

where K_B is Boltzmann's constant, h is Planck's constant, and F_i are the partition functions describing the energy associated with each degree of freedom (i.e., translation, rotation, and vibration) of each component. Because the partition functions are computed upon first-principles and depend on the molecular masses of the components, the effect of $A'/A = F_{C'} F_S / F_C F_{S'}$ on α is fully predictable. Bigeleisen and Wolfsberg [1958] predicted in this way the isotopic effects of several stable isotopes involved in unimolecular reactions. The calculation of isotopic effects for bimolecular reactions of multiatomic molecules such as in N_2O production and consumption reactions investigated here are more difficult to assess. There are two aspects that prevents us from computing A'/A. In the specific case of N_2O production from NO_3^-, the three reduction steps $NO_3^- \rightarrow NO_2^- \rightarrow NO \rightarrow N_2O$, each associated with one specific enzyme (i.e., nitrate reductase, nitrite reductase and nitric oxide reductase), are aggregated and simplified into one single reduction reaction operated by one enzyme that combines the functioning of the three enzymes. This simpli-

fication, however, does not invalidate the model proposed here which implicitly assumes that the enzyme concentration, E, is the sum of the concentration of the three enzymes, while the three reactions are implicitly assumed to occur simultaneously and with the same rates. In the case of $N_2O \rightarrow N_2$ reduction only one reaction is involved and it is catalyzed by the nitrous oxide reductase enzyme. While the N_2O consumption reaction could be the right candidate to assess the effect of A'/A from the partition functions, the complicated network of long-chained proteins of the enzyme structure [Rosenzwieg, 2000] makes particularly difficult to determine the translational, rotational, and vibrational energies required to calculate F_E, F_C, and $F_{C'}$. The second aspect that prevent us from computing the effect of A'/A on the isotopic effect is related to the fundamentals of the derivation of the Michaelis-Menten and Eyring equations. Both equations are essentially equilibrium theories by virtue of the equilibrium that is assumed to link the complex and reactant concentrations. The equilibrium assumption implies that the rate of production of P is much slower than the time scale required by the reactants to form the complex and that any variation in reactant concentrations is instantaneously transferred to the complex concentration, which increases or decreases concordantly. The Haldane-Briggs' quasi-steady-state assumption, instead, states that the complex concentration is time invariant. Because it does not imply equilibrium between complex and reactants, the concentrations of the complex does not change in response to a change in reactant concentration. The theory of rate processes that Eyring proposed to describe the rate of chemical reactions leading to the partition functions may therefore not be accurate, or conceptually correct, in a system which is at steady state as compared to a system which is at equilibrium. The Eyring equation has not been proven yet to hold valid under the

Haldane-Briggs' assumption. The correct application of the Eyring equation in the case of transient Michaelis-Menten kinetics is a fortiori more arguable than for the quasi-steady-state Michaelis-Menten kinetics. Although the Eyring equation cannot be rigorously used in this instance, it is likely that isotopic effects will depend not only on the difference in energy barrier ($E'_a - E_a$) but also on the ratio between the frequency factors A'/A and, consequently, on the corresponding partition functions. The crucial point to this end is therefore that of deriving a form of the Eyring equation for quasi-steady-state and transient complex concentration, and determine whether the expressions for the frequency factors A and A' maintain the current form of Eqs. (24) or require rewriting. We conclude that, currently, a thermodynamic analysis of the k_i and k'_i values based on the activation energy introduced with Arrhenius' law is mathematically consistent with the chemistry of the processes, while an interpretation using the Eyring equation is not appropriate at the present state of development.

Finally, the results described in Section 3 and summarized here for point-scale modeling can have important consequences for interpreting isotopic signatures at small scales such as in laboratory investigations. Future applications of isotope movement throughout the large-scale ecosystem may also benefit from the modeling approach described here, which may become important to determine soil nutrient cycling, turnover rates, accumulation, escape pathways, and global spatial distributions.

5. Conclusions

Our understanding of isotopic fractionation is limited even in simple biogeochemical systems. In this paper, we have shown that: (i) transient Michaelis-Menten-Monod kinetics in competitive complexation was superior to quasi-steady-state and first-order kinetics

when predicting concentrations and isotopic compositions over time, and that (ii) transient Michaelis-Menten-Monod kinetics explained observed non-steady isotopic effects. The higher accuracy of the method was linked to the transient assumption by which the fractionation factor becomes variable with the isotopic compositions of complex and substrate over time. The approach presented here in describing the competitive consumption of isotopologue substrates may imply a substantial revision in using first-order kinetics and the Rayleigh equation as well as the quasi-steady-state Michaelis-Menten-Monod kinetics for interpretation of isotopic signatures.

Acknowledgments.

The authors thank Christof Meile and Bruce Hungate for their comments and suggestions on the first development of the models. This work was supported by Laboratory Directed Research and Development (LDRD) funding from Berkeley Lab, provided by the Director, Office of Science, of the U.S. Department of Energy under contract DE-AC02-05CH11231.

References

Atkins P.W., (1998), *Physical Chemistry*, 6th ed., Freeman, Oxford University Press, pp 999.

Connors K.A., (1990), *Chemical kinetics: The study of reaction rates in solution*, Wiley-VCH, pp. 480.

Bigeleisen J. and M. Wolfsberg (1958), Theoretical and experimental aspects of isotope effects in chemical kinetics, Adv. Chem. Phys. 1, 15-76.

Conrad R. (1996), Soil Microorganisms as controllers of atmospheric trace gases (H2, CO, CH4, OCS, N_2O and NO), Microbiological Reviews Dec., 609-640.

Dixon M. and E.C. Webb, (1958), *Enzymes*, Academic Press, Inc., New York, pp 782.

Eyring H., (1935), The activated complex and the absolute rate of chemical reactions, Chemical Reviews 17(1), 65-77.

Eyring H., (1935), The activated complex in chemical reactions, Journal of Chemical Physics 3(2), 107-115.

Glasstone S., K.J. Laidler and H Eyring, (1941), The theory of rate processes, McGraw-Hill, pp. 611.

Groffman P.M., M.A. Altabet, J.K. Bohlke, K. Butterbach-Bahl, M.B. David, M.K. Firestone, A.E. Giblin, T.M. Kana, L.P. Nielsen and M.A. Voytek, (2006), Methods for measuring denitrification: Diverse approches to a difficult problem, Ecological Applications 16(6), 2091-2122.

Haldane J.B.S. (1930), *Enzymes*, London, New York, Longmans, Green, pp 235.

Hunkeler D. and R. Aravena (2000), Evidence of Substantial Carbon Isotope Fractionation among Substrate, Inorganic Carbon, and Biomass during Aerobic Mineralization of 1,2-Dichloroethane by Xanthobacter autotrophicus, Applied Environmental Microbiology, 66(11), 4870-4876.

Knowles R. (1982), Denitrification, Microbiological Review, Mar., 43-70.

Laidler K.J. (1955), Theory of the transient phase in kinetics, with special reference to enzyme systems, Can. J. Chem. 33, 1614-1624.

Laidler K.J., (1965), *Chemical kinetics*, McGraw-Hill, pp. 566.

Li C., S. Frolking and T. Frolking, (1992), A model of nitrous oxide evolution from soil driven by rainfall events: 1. Model structure and sensitivity, J. Geophys. Res. 97, 59-76.

Mariotti A., J.C. Germon, P. Hubert, P. Kaiser, R. Letolle, A. Tardieux, P. Tardieux, (1981), Experimental determination of nitrogen kinetic isotope fractionation - Some principles - Illustration for the denitrification and nitrification processes, Plant and Soil 62(3), 413-430.

Menyailo O.V. and B.A. Hungate, (2006), Stable isotope discrimination during soil denitrification: Production and consumption of nitrous oxide, Global Biogeochemical Cycles 20(GB3025), doi:10.1029/2005GB002527.

Monod J., (1949), The growth of bacterial cultures, Annu. Rev. Microbial 3, 371-394.

Mosier A.G. (1998), Soil processes and global change, Biol. Fertil. Soils 27, 221-229.

Papadopulos & Associates, Inc., www.sspa.com/pest.

Perez T., Garcia-Montiel D., Trumbore S., Tyler S¿, De Camargo P., Moreira M., Piccolo M. and Cerri C., (2006), Nitrous oxide nitrification and denitrification ^{15}N enrichment factors from amazon forest soils, Ecological Applications 16(6), 2153-2167.

Rosenzwieg A., (2000), Nitrous oxide reductase from CuA to CuZ, Nature Structural Biology 7, 169-171.

Sprent J., (1987), The ecology of the nitrogen cycle, Cambridge University Press, New York, pp 150.

Toyoda S., Mutobe H., Yamagishi H., Yoshida N. and Tanji Y., (2005), Fractionation of N_2O isotopomers during production by denitrifier, Soil Biology and Biogeochemistry 37, 1535-1545.

Vitousek P.M., G. Shearer, and D.H. Kohl, (1989), Foliar 15-N natural abundance in Hawaiian rainforest: Patterns and possible mechanisms, Oecologia, 78, 383-388.

Vitousek P.M., J.D. Aber, R.W. Howarth, G.E. Linkens, P.A. Matson, D.W. Schindler, W.H. Schlesinger and D.G. Tilman, (1997), Human alteration of the global nitrogen cycle: sources and consequences, Ecological Applications 7(3), 737-750.

Wrage N., G.L. Velthof, M.L. van Beusichem and O. Oenema, (2001), Role of nitrifier denitrification in the production of nitrous oxide, Soil Biology and Biochemistry 33, 1723-1732.

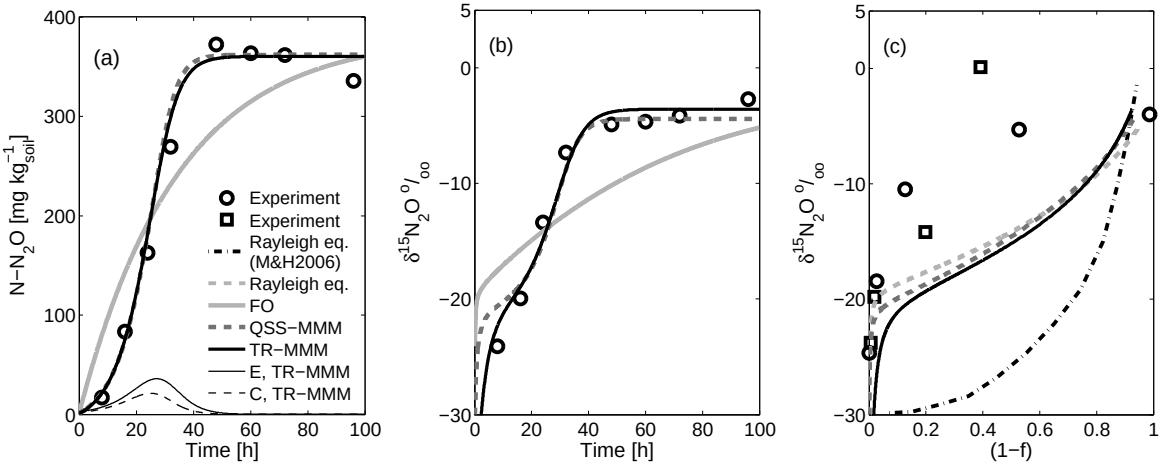

Figure 1. (a) observed and predicted N_2O concentration over time during N_2O production from NO_3^-; (b) and (c) observed and predicted N_2O product isotope composition over time and as a function of consumed substrate $(1 - f)$. Experimental data and the Rayleigh equation represented by the dot-dashed line are redrawn from Menyailo and Hungate [2006]. Data points in (a) and (b) are averages of multiple replicates and do not show appreciable variance (see Figure 1A and C in Menyailo and Hungate [2006]), while data points in (c) represent two replicates where $(1-f)$ was estimated from the remaining substrate (see Figure 2A in Menyailo and Hungate [2006]).

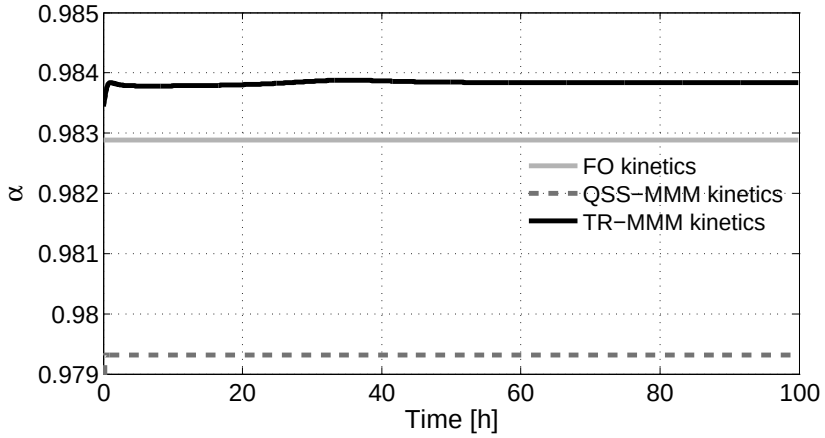

Figure 2. Fractionation factor, α, computed with first-order (FO) kinetics, quasi-steady-state Michaelis-Menten-Monod kinetics (QSS-MMM), and transient Michaelis-Menten-Monod kinetics (TR-MMM) during N_2O production.

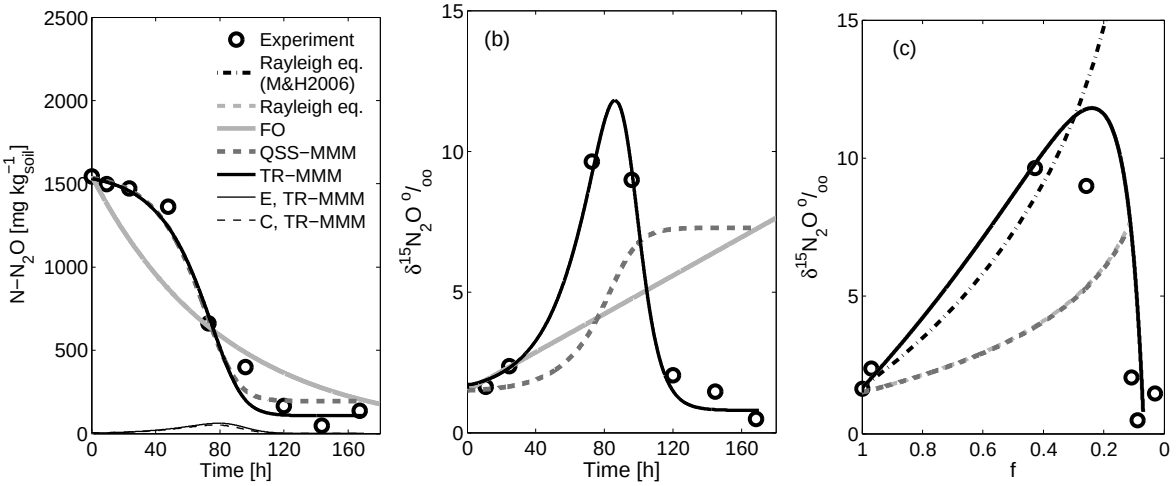

Figure 3. (a) observed and predicted N_2O concentration over time during N_2O consumption into N_2, (b) and (c) observed and predicted N_2O product isotope composition over time and as a function of remaining substrate f. Experimental data and the Rayleigh equation represented by the dot-dashed line are redrawn from Menyailo and Hungate [2006]. Data points in (a) were originally expressed with the unit of [ppm], while here they are represented with the unit of [mg kg^{-1}_{soil}], and were computed using a soil mineral density of 2500 kg m^{-3}, a porosity of 0.4, and soil water saturation of 0.6. Data points in (a), (b), and (c) are averages of several replicates (see Figure 3A and B in Menyailo and Hungate [2006]), Data points in (c) report the full set of experimental values, including the last three points of (b) (see Figure 5A in Menyailo and Hungate [2006]).

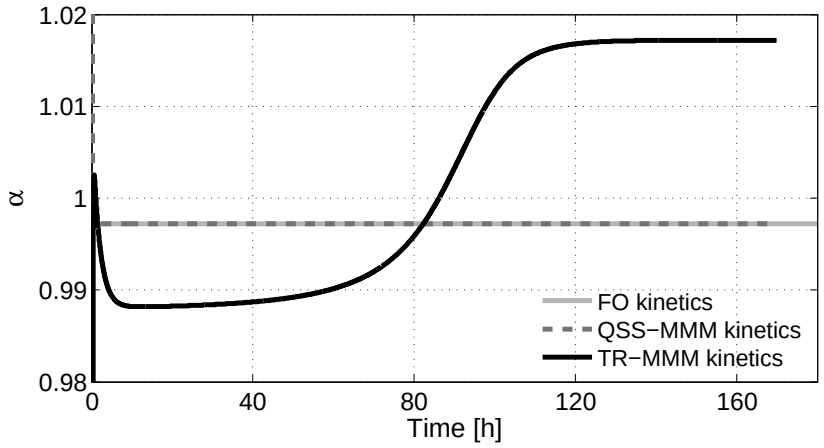

Figure 4. Fractionation factor, α, computed with first-order (FO) kinetics, quasi-steady-state Michaelis-Menten-Monod kinetics (QSS-MMM), and transient Michaelis-Menten-Monod kinetics (TR-MMM) during N_2O consumption.

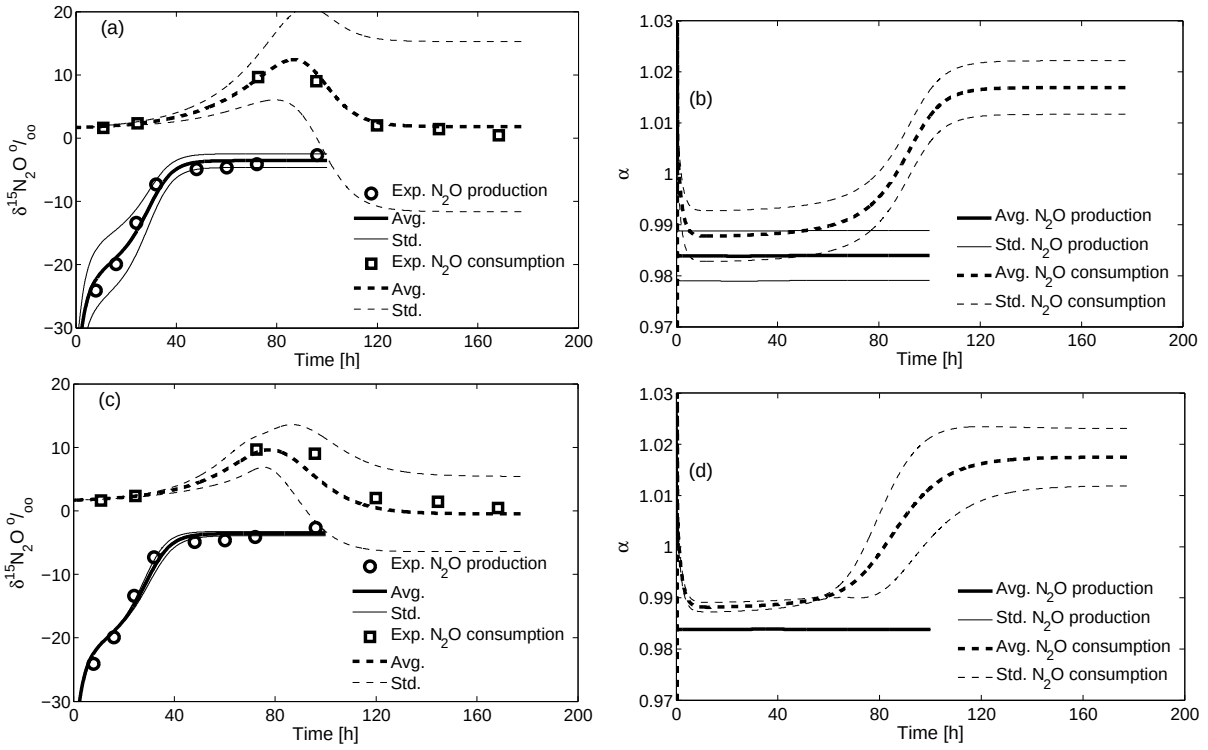

Figure 5. (a) and (b) represents the mean (Avg.) and standard deviation (Std.) of Monte Carlo sensitivity analysis of $\delta^{15}N_2O$ and fractionation factor α over time for imposed variances of $\pm 5‰$ in the k_i' rates during N_2O production and consumption. (c) and (d) represent the mean and standard deviation of Monte Carlo sensitivity analysis of $\delta^{15}N_2O$ and fractionation factor α over time for imposed variances of $\pm 1\%$ in the microbial biomass parameters z and β during N_2O production and consumption. Modeling results were obtained with the transient Michaelis-Menten-Monod kinetics (TR-MMM), and were compared with experimental data redrawn from Menyailo and Hungate [2006].

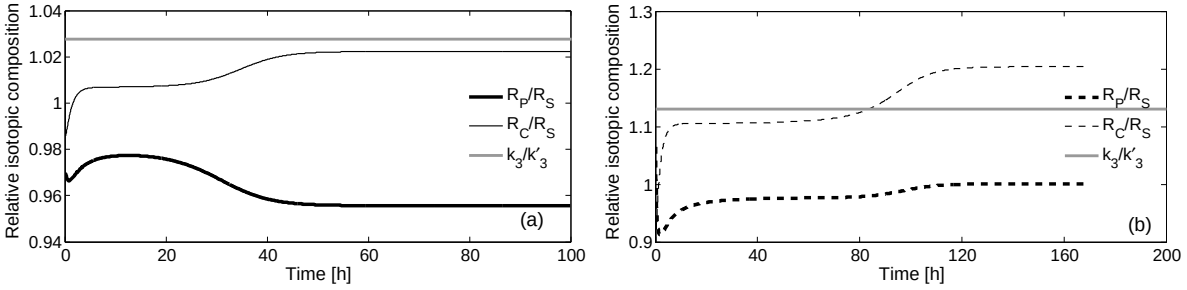

Figure 6. (a) and (b) isotopic composition of complex, R_C, and product, R_P, relative to the composition of the substrate, R_S, computed with the TR-MMM kinetics for N_2O production and consumption, respectively.

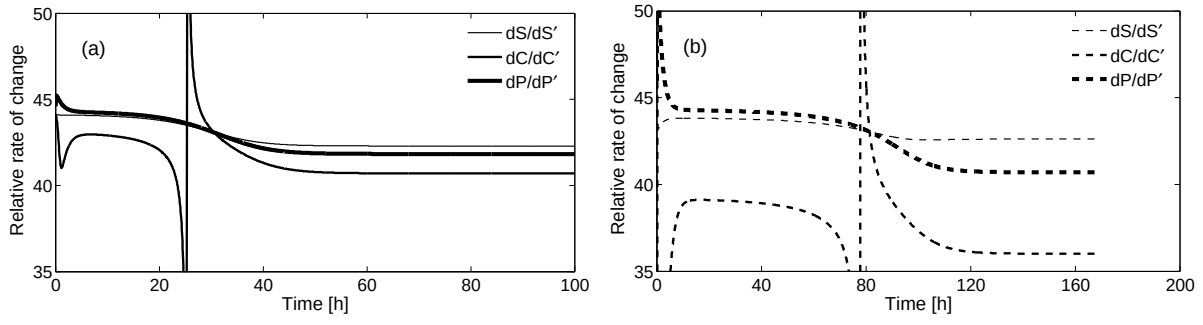

Figure 7. (a) and (b) representations of the relative rates of change of substrates, $\mathrm{d}S/\mathrm{d}S'$, complexes, $\mathrm{d}C/\mathrm{d}C'$, and products, $\mathrm{d}P/\mathrm{d}P'$, for the two experiments of N_2O production and consumption, respectively, computed with the TR-MMM kinetics. The symbols S and S', and P and P' stay for $^{14}NO_3^-$ and $^{15}NO_3^-$, and for $^{14}N_2O$ and $^{15}N_2O$ in panel (a), and for $^{14}N_2O$ and $^{15}N_2O$, and $^{14}N_2$ and $^{15}N_2$ in panel (b), respectively.

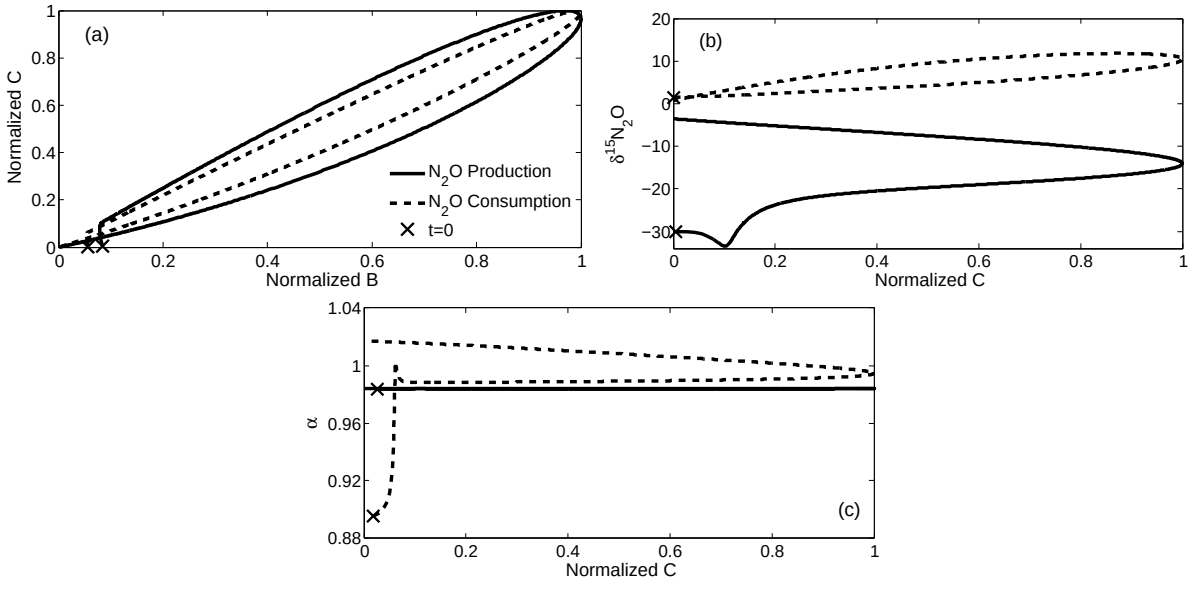

Figure 8. (a) representation of the normalized complex concentration C as a function of the normalized microbial biomass concentration B. (b) representation of the isotopic composition $\delta^{15}\mathrm{N_2O}$ as a function of the normalized complex concentration C. (c) representation of the fractionation factor, α as a function of the normalized complex concentration C.

Table 1. Summary of parameters used in (*a*) first-order kinetics (FO), (*b*) quasi-steady-state Monod kinetics (QSS-MMM), and (*c*) transient Monod kinetics (TR-MMM) in the two tests of N_2O production and consumption. The parameters bracketed in the first column were calibrated while all others were obtained from the experiments. The value of z was assigned arbitrarily. The biomass parameters z and β, and the initial concentrations S_0, C_0, P_0, and B_0, and isotopic compositions $R_{S,0}$, $R_{C,0}$, and $R_{P,0}$ were identically applied to each model, were the reference isotope composition, $R_{std} = 2.305 \cdot 10^{-2}$ was used. The parameters K and K' within *-* in the TR-MMM kinetics were not calibrated but calculated a posteriori as $K^* = (k_2 + k_3)/k_1$ and $K'^* = (k'_2 + k'_3)/k'_1$ for comparison with K and K' of the QSS-MMM kinetics. The values of the parameters k_i and k'_i are expressed with a precision of four digits owing to the model sensitivity to these values (Section 3.6).

			N_2O production			**N_2O consumption**		
			FO	QSS-MMM	TR-MMM	FO	QSS-MMM	TR-MMM
(k)	$[s^{-1}]$	$\cdot 10^{-6}$	8.0757	-	-	3.3397	-	-
(k')	$[s^{-1}]$	$\cdot 10^{-6}$	7.9375	-	-	3.3303	-	-
(k_1)	$[mg\ kg_{soil}^{-1}\ s^{-1}]$	$\cdot 10^{-6}$	-	-	2.0713	-	-	1.7806
(k'_1)	$[mg\ kg_{soil}^{-1}\ s^{-1}]$	$\cdot 10^{-6}$	-	-	2.0369	-	-	1.5947
(k_2)	$[s^{-1}]$	$\cdot 10^{-6}$	-	-	1.6604	-	-	3.4703
(k'_2)	$[s^{-1}]$	$\cdot 10^{-6}$	-	-	1.5381	-	-	1.4936
(k_3)	$[s^{-1}]$	$\cdot 10^{-4}$	-	1.8831	2.0846	-	1.4949	1.4488
(k'_3)	$[s^{-1}]$	$\cdot 10^{-4}$	-	1.7262	2.0284	-	1.4720	1.2818
(K)	$[mg\ kg_{soil}^{-1}]$		-	76.81	$^*101.44^*$	-	150.48	$^*100.85^*$
(K')	$[mg\ kg_{soil}^{-1}]$		-	71.90	$^*100.33^*$	-	148.59	$^*89.74^*$
z	$[mg\ mg^{-1}]$		-	0.01	0.01	-	0.01	0.01
(Y)	$[mg\ mg^{-1}]$		-	95.631	95.63	-	95.63	95.63
(β)	$[s^{-1}]$	$\cdot 10^{-4}$	-	1.1635	1.1635	-	1.1635	1.1635
S_0	$[mg\ kg_{soil}^{-1}]$		380	380	380	1500	1500	1500
C_0	$[mg\ kg_{soil}^{-1}]$		-	10^{-10}	10^{-10}	-	10^{-10}	10^{-10}
P_0	$[mg\ kg_{soil}^{-1}]$		10^{-10}	10^{-10}	10^{-10}	10^{-10}	10^{-10}	10^{-10}
B_0	$[mg\ kg_{soil}^{-1}]$		-	300	300	-	350	350
$R_{S,0}$	$[-]\cdot 10^{-2}$		2.305	2.305	2.305	2.459	2.459	2.459
$R_{C,0}$	$[-]\cdot 10^{-2}$		-	2.305	2.305	-	2.459	2.459
$R_{P,0}$	$[-]\cdot 10^{-2}$		2.24	2.24	2.24	2.459	2.459	2.459